Comparison of Photocatalytic Activities of Two Different Dyes Using Pt-Modified TiO$_2$ Nanoparticles under Visible Light

Akbar Jodat[1*] , Mehri Alizad Nikjoo[2], Mahboubeh Ghamkhari[1]

[1]*Laboratory of Chemistry, Shahindezh Branch, Islamic Azad University, Shahindezh, Iran*
[2]*Department of Chemistry, Ahar Branch, Islamic Azad University, Ahar, Iran*

Abstract

The photocatalytic degradation of Acid Red 91 (AR91) and Acid Yellow 23 (AY23) with different molecular structures and different substitute groups using Pt modified TiO$_2$ (Pt-TiO$_2$) nanoparticles was investigated in the presence of visible light irradiation. Pt-TiO$_2$ nanoparticles were prepared with photodiposition method (PD) and characterized by X-ray diffraction (XRD), scanning electron micrographs (SEM), energy dispersive X-ray micro analysis (EDX), transmission electron microscope (TEM), and UV-vis diffuse reflection spectra (DRS) techniques. The DRS results indicated that the deposition of platinum on TiO$_2$ promoted the optical absorption in the visible region and made it possible to be excited by visible light. Pt-modification of the surface of TiO$_2$ increased photocatalytic activity under visible light irradiation, depending on dye structure (functional group and reactivity of dyes). By comparing the removal efficiency of AR91 and AY23 at the similar conditions, it was observed that the photodegradation rate of AR91 was faster than that of AY23. In conclusion, photocatalytic mineralization of the dyes was monitored by total organic carbon (TOC) decrease. Above 82 and 94% mineralization of AY23 and AR91 was observed using 2 h irradiation.

Keywords: *Photocatalytic degradation, Acid Red 91, Acid Yellow 23, Pt modified* TiO$_2$*, Photodeposition, Visible light.*

Corresponding author: *Akbar Jodat, Laboratory of Chemistry, Shahindezh Branch, Islamic Azad University, Shahindezh, Iran. Email: akbarjodat@gmail.com, Tel: +984446221022; Fax: +984446229092.*

Introduction

The presence of harmful organic pollutants in wastewater effluents causes serious environmental problems. Dyes as water pollutants are nonbiodegradable and releasing them into the environment poses a significant threat to the surrounding ecosystems. Color removal from effluent is one of the most difficult requirements faced by the textile finishing, dye manufacturing, and pulp and paper industries. Due to this, organic dyes are one of the main industrial wastewater pollutions [1, 2].

Among the dyes, xanthene dyes have many uses in textile, paper, food, cosmetics, pharmaceuticals, medicine and biological staining, due to superior dyeing and coloring properties. These dyes exhibit poor biodegradability and some of them are toxic. Other groups of organic dyes including azo dyes have also some serious environmental impacts. Acid Red 91 (AR91) is a xanthene dye in the form of triclinic crystals, water-soluble, distinctly bluish shade and highly toxic. Although Acid Yellow 23 (AY23) is used as a cosmetic, drug, and food coloring dye it is considered highly toxic for humans due to high amounts in industrial effluents because of its high solubility [3, 4]. Typical techniques include the conventional methods such as biodegradation, filtration, coagulation, electrocoagulation and adsorption [5-8]. Due to the limited effectiveness of conventional wastewater treatments, advanced oxidation processes (AOPs) can be explored as an alternative in order to reduce the dye compounds [9]. Among these processes, photocatalytic method (TiO_2) can play an important role in new technologies of water and wastewater purification.

Photocatalytic degradation techniques utilizing visible light are quite safe, cost effective and easy to handle, therefore, has gaining more attention as compared to UV light assisted photocatalytic degradation of organic molecules but very little attention has been paid on degradation process utilizing visible light. In order to solve these problems, there have been many efforts to make a TiO_2 photocatalyst that would be active under visible irradiation.

Various techniques have been employed to make them absorb photons of lower energy as well. These techniques include surface modification via organic materials [10] and semiconductor coupling [11], band gap modification by creating oxygen vacancies and oxygen sub-stoichiometry [12], by nonmetals including co-doping of nonmetals [13] and metals doping [14]. Modification of TiO_2 nanoparticles was done with transition metals [15], lanthanide metals [16], alkaline metals [17], non metals [18] and etc. Earlier studies have revealed that the photocatalytic activity of TiO_2 nanoparticles can be improved significantly by modification with noble

metals such as Pt [19], Au [20], Pd [21] and Ag [22]. Modification TiO_2 with noble metals, such as Pt, Pd and Au can overcome the aforementioned deficiency. Deposition of noble metals like Ag, Au, Pt and Pd on the surface of TiO_2 enhances the photocatalytic efficiency under visible light by acting as an electron trap, promoting interfacial charge transfer and therefore delaying recombination of the electron-hole pair [23]. However, these noble metals are too expensive to be utilized in industrial scale. Among these, Pt modified TiO_2 are expected to become commercially promising photocatalysts due to their high activity. The Pt deposited on the surface of TiO_2 can significantly absorb visible light [24-26].

The effect of Pt on photocatalytic activity under visible-light irradiation has been studied by several research groups [26-29]. Nevertheless, there are rare studies concerning the photocatalytic degradation of two dyes with different molecular structure using Pt-TiO_2 catalyst under visible-light irradiation [26].

To our knowledge, there is no systematic study dealing with comparative photocatalytic removal of a xanthene and an azo dye with different molecular structure under visible-light irradiation using Pt-TiO_2 nanoparticles obtained via photodiposition (PD) method. The present work is focused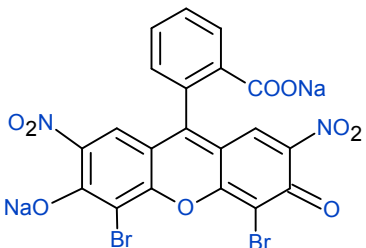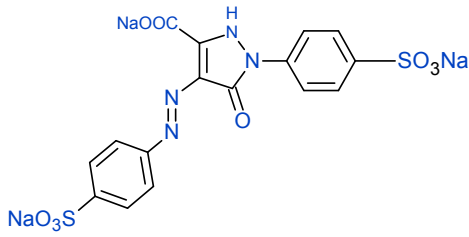 on the comparative photocatalytic degradation of AR91 (a xanthene dye) and AY23 (an azo dye) with different molecular structures using pure TiO_2 and Pt modified TiO_2 nanoparticles obtained via PD method in the presence of visible-light irradiation. Pt-TiO_2 nanoparticles have been characterized using XRD, SEM, EDX, TEM and DRS techniques. Along the way, the effects of various operational parameters (platinum concentration, photocatalyst loading, initial dye concentration, light intensity, and calcination temperature) have been evaluated to maximize the degradation of AR91 and AY23 under investigation. Extent of photodegradation and mineralization has been measured by using UV-vis spectrometer and total organic carbon (TOC) analyzer, respectively.

Experimental

Materials

Hexachloroplatinic acid (H_2PtCl_6 98%) and H_2SO_4 were obtained from Merck. TiO_2-P25 Degussa (80% anatase, 20% rutile; BET area 50 m^2/g; primary size 21 nm) were used as a supporting material. AR91 and AY23 were purchased from Aldrich and ACROS organics, respectively. Structure and other characteristics of the two dyes are given in Table 1.

Table 1. Structure and characteristics of AR91 and AY23.

Chemical structure		
	Molecular formula	$C_{20}H_6Br_2N_2Na_2O_9$
	Other names	C.I. acid red 91; eosin bluish, saffrosine, eosin scarlet
	IUPAC name	4',5'-Dibromo-3',6'-dihydroxy- 2',7'-dinitro-spiro[isobenzofuran-1(3H), 9'-[9H]xanthen]- 3-one,disodium salt
	C.I. number	45400
	λ_{max} **(nm)**	515
	M_w **(g/mol)**	624.06
	Molecular formula	$C_{16}H_9N_4Na_3O_9S_2$
	Other names	C.I. acid yellow 23, C.I. food yellow 4, E102, FD&C yellow 5
	IUPAC name	4,5-Dihydro-5-oxo-1-(4-sulfophenyl)-4-[(4-sulfophenyl)azo]-1H-pyrazole-3-carboxylic acid trisodium
	C.I. number	19,140
	λ_{max} **(nm)**	429
	M_w **(g/mol)**	534.385

The preparation of platinum doped TiO₂ nanoparticles

In the PD method, Pt modified TiO_2 was prepared by photoreducing Pt^{2+} ions to Pt metal on the TiO_2 surface. For preparation of Pt-TiO_2 nanoparticles, proper amount of TiO_2-P25 was added into 100 ml of deionised water and required amount of H2PtCl6 for loading was added into the suspension of TiO_2. The pH of TiO_2 suspension was adjusted to 3. Then the mixture was irradiated under UV light (30 W, λ_{max} =254 nm) for 3 h and then dried at 100 ºC for 12 h. The dried solids were calcinated at 300ºC for 3 h in a furnace.

Photoreactor and procedure

For investigation of the photocatalytic activity of Pt-TiO_2 nanoparticles, a solution containing known concentration of dye (AR91 or AY23) and nanoparticle (pure or Pt-modified TiO_2 nanoparticles) was allowed to equilibrate for 30 min in the darkness and then 100 mL of the prepared suspension was transferred into a borosilicate petri dish (12 cm diameter and 2.5 cm height) as a photoreactor. The reaction mixture was stirred vigorously under the illumination of visible light from top of the solution using a visible lamp (OSRAM, 500 W; 125 klux). For kinetic studies, at certain reaction

intervals, 5mL of sample was withdrawn. To remove the Pt-TiO$_2$ particles from the reaction media, the solution was centrifuged for 15 min at 5,000 rpm. The concentration of AR91 and AY23 was determined with a UV-vis spectrophotometer at 515 and 429 nm, respectively. Calibration plot based on Beer-Lambert's law was established by relating the absorbance to the concentration. All the photodegradation experiments were carried out at room temperature with pH of about 6.5, which is the natural pH of the reaction medium. All the concentration profiles can be correlated to irradiation time by the following exponential function with good agreement:

$$C = C_0 \exp(-k_{app}t) \qquad (1)$$

Therefore the photocatalytic decolorization of AR91 and AY23 is pseudo-first-order reaction and its kinetics may also be expressed as:

$$-\ln\frac{C}{C_0} = k_{app}t \qquad (2)$$

where k$_{app}$ is the apparent rate constant (min^{-1}), t is the irradiation time (min), C$_0$ is the initial concentration of dye (mg/L) and C is the concentration of dye (mg/L) at time t [30].

Characterization and analytical methods
The crystalline phase of nanoparticles were analyzed by X-ray diffraction measurements by using Siemens XRD-D5000 (λ=0.154 nm). Morphological studies were conducted using a scanning electron microscopy (SEM, Viga

II, 3×105, USA) equipped with a probe for the energy dispersive X-ray micro analysis (EDX). The surface properties were observed under TEM (PHILIPS CM 10-100 keV). Ultraviolet/visible diffuse reflectance spectra (DRS) were taken on AvaSpec-2048 TEC spectrometer. An ultrasonic bath from Elma (model T 460/H, Singen, Germany) was used for sonication of the samples. A visible lamp (OSRAM, 500 W; 125 klux) was used as the excitation source. Additionally, a UV-vis spectrophotometer (Ultrospec 2000, England) was used for measurement of the concentration of AR91 and AY23. Finally, concentration of TOC in the solution was measured using a TOC analyzer (Shimadzu, TOC-VCSH).

Results and Discussion
Catalyst characterization
XRD analysis
The XRD patterns of the TiO$_2$ and 1 wt% Pt-TiO$_2$ photocatalysts is shown in Figure 1. Both catalysts show the dominant anatase peaks at 2θ = 25.2°, 38°, 48.2°, 55° and 62.5° and the small fraction of rutile at 2θ =27.5°, 36°, 54° and 69°. It is worth noting that no peaks of Pt were observed in the case of Pt-TiO$_2$, suggesting that the platinum is merely placed on the surface of the crystals [31]. The X-ray diffraction patterns of platinum modified TiO$_2$ samples almost coincide with that of pure TiO$_2$ and show no diffraction peaks due to platinum species. There is no change in the

crystal structure upon doping of Pt. Since there are no diffraction patterns characteristic of modified metal in the XRD, these metal sites are expected to be below the visibility limit of X-ray analysis [32].
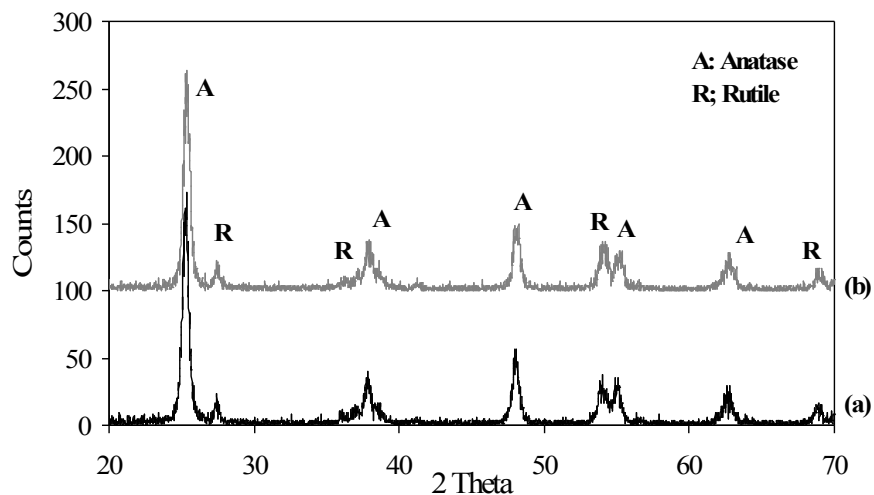

Figure 1. XRD patterns of: a) TiO_2, and b) 1 wt% Pt-TiO_2.

SEM and EDX analysis

Figures 2a and 2b show the scanning electron microscopy (SEM) micrographs of the TiO_2-P25 and 1wt% Pt-TiO_2. Comparison of the SEM micrographs of pure TiO_2 and Pt-TiO_2 nanoparticles proved that, loading of Pt nanoparticles did not affect the spherical shape of TiO_2 nanoparticles[24]. We have also performed EDX analysis on the Pt-modified TiO_2 catalyst (Figure 2c). The presence of loaded Pt on the TiO_2 nanoparticles also was confirmed by this analysis.
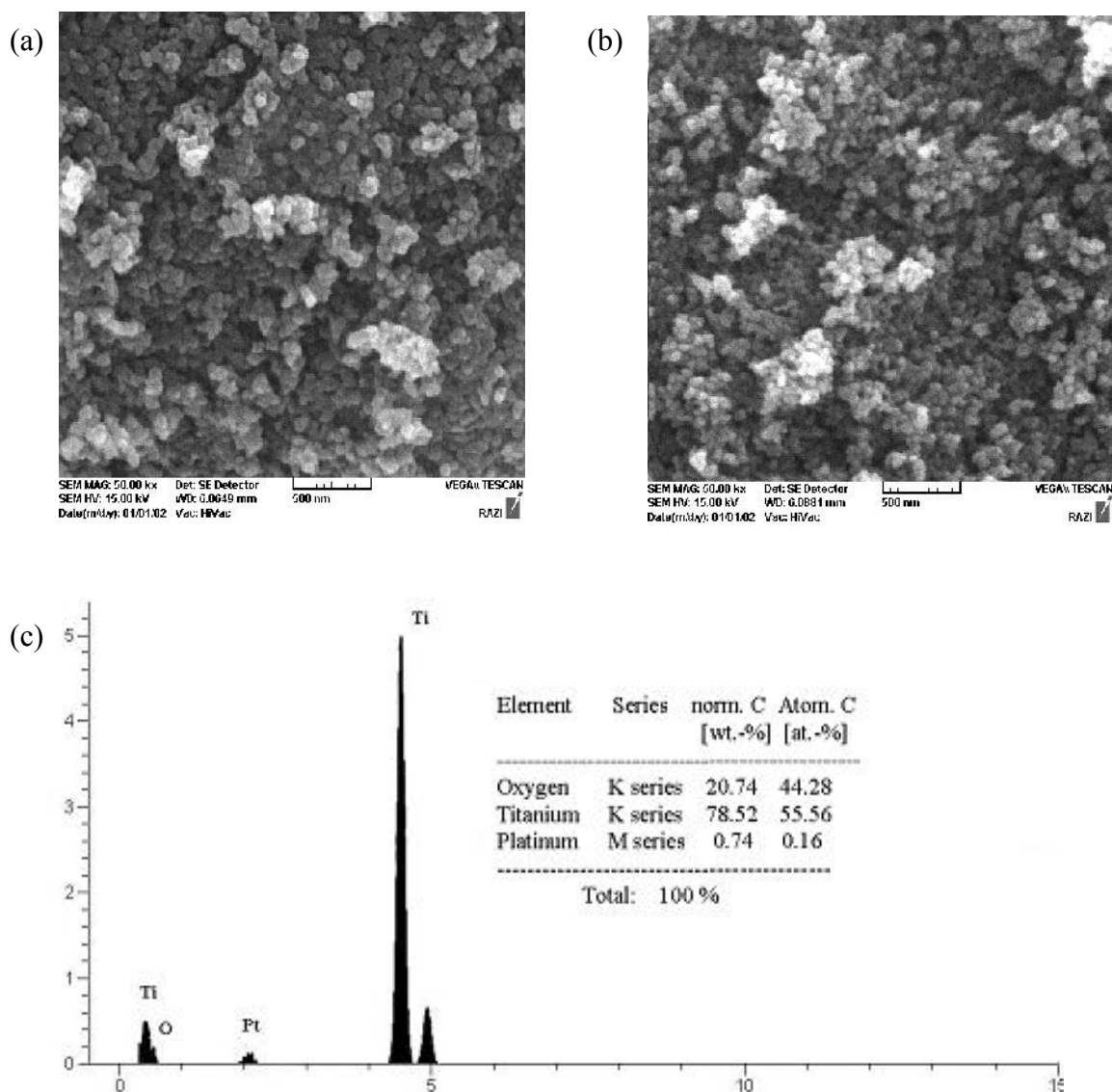
(a)

(b)

(c)

Element	Series	norm. C [wt.-%]	Atom. C [at.-%]
Oxygen	K series	20.74	44.28
Titanium	K series	78.52	55.56
Platinum	M series	0.74	0.16

Total: 100 %

Figure 2. SEM pictures of: TiO_2 (a); 1 wt% Pt–TiO_2 (b) and EDX diagram of 1 wt.% Pt-TiO_2 nanoparticles (c).

TEM measurement

The particle sizes of the Pt nanoparticles were measured from the TEM micrographs, Figure 3 shows the TEM micrograph of Pt loaded TiO_2 catalyst. The average particle size of Pt-TiO_2 was found to be 20-25 nm. The shape and size of the titania crystallites (TiO_2-P25) were unchanged as a result of surface modification by platinum particles. Platinum particles (black dots indicated) were located on the surface of the individual TiO_2 nanoparticles. Also, there is a possibility for the platinum to be incorporated into the interstitial positions of the semiconductor particles [33].
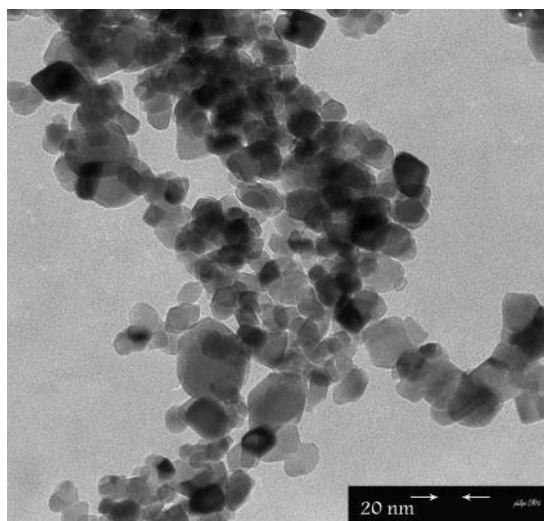
Figure 3. TEM micrograph of 1% Pt-TiO$_2$ nanoparticles.

Diffuse reflectance UV-vis spectra (DRS)

Figure 4a represents the UV-vis absorption spectra of pure TiO$_2$ and Pt-TiO$_2$ nanoparticles in the range of 200-900 nm. Compared with the bare TiO$_2$ nanoparticles, Pt-TiO$_2$ nanoparticles show an absorption in the region of 450-492 nm. Therefore, the platinum species on the sample may play a role as the sensitizer for visible-light absorption. Li and Li [26] also confirmed the enhancement of visible optical absorption due to the presence of Pt, Pt(OH)$_2$, and PtO$_2$ has been proven by UV-vis reflectance spectra. The major role of Pt incorporated on TiO$_2$ could be attributed to accelerate the formation of superoxide radical anion O$_2^-$ and also decrease the probability of recombination of electrons and holes by scavenging the electrons in the conduction band by Pt nanoparticles. The band gap energy of catalysts can be calculated by the following equation:

$$\alpha(h\nu) = B(h\nu - E_g)^{1/2} \qquad (3)$$

where α is optical absorption coefficient, B is a constant dependent on the transition probability, h is the Plank's constant and ν is the frequency of the radiation. The E$_g$ values were calculated from Figure 4 (b) by plotting $(\alpha h\nu)^2$ versus hν, followed by extrapolation of the linear part of the spectra to the energy axis [34].

The calculated band gap (E$_g$) energies were 3.16 eV for pure TiO$_2$-P25 and 2.75 eV for 1 wt% Pt-TiO$_2$. Results indicate that Pt loading on TiO$_2$ surface decreased optical band gap energy, whereas decrease in E$_g$ value for Pt-TiO$_2$ is higher than for pure TiO$_2$ catalyst. This lower energy value has been attributed to the strong absorption in visible region due to localized levels existing in the forbidden gap because of Pt loading. Upon irradiation with visible light electron-hole pair is generated

within the effective band gap, i.e., electron transition takes place from the new additional valence state to conduction state. This transition requires smaller excitation energy as compared to the native band gap (3.16 eV) of TiO_2, therefore it can be used as an efficient photocatalyst under visible light irradiation [35].
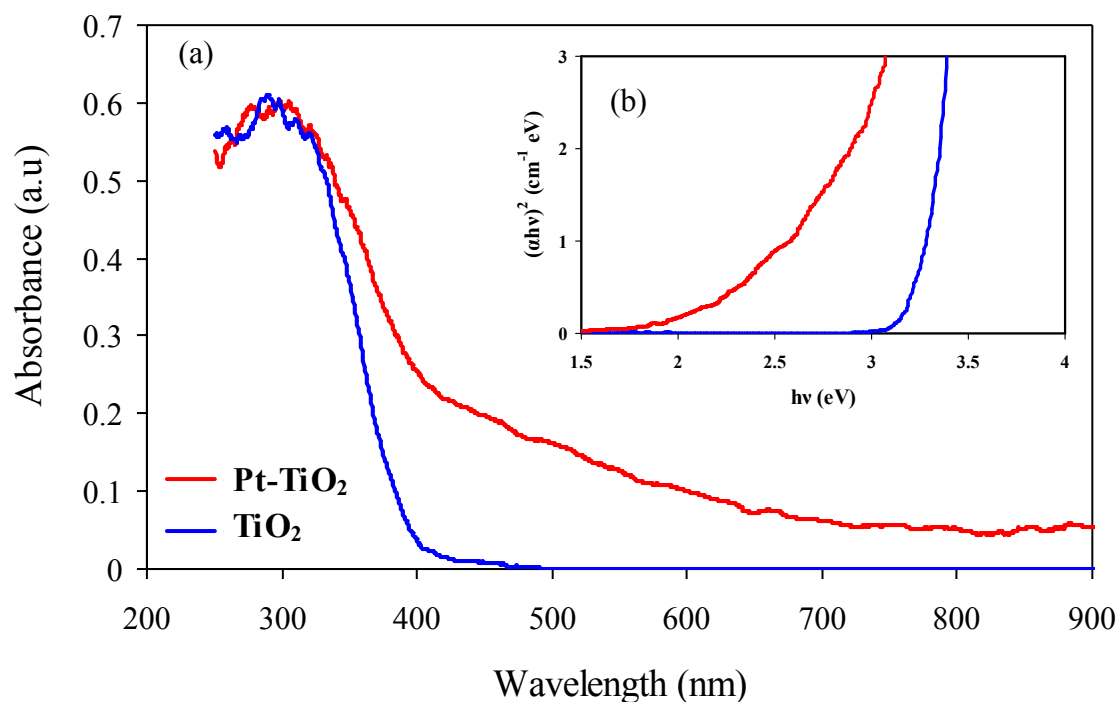

Figure 4. UV-vis absorption spectra for pure TiO_2 and Pt-TiO_2 nanoparticles (a) Plot of $(\alpha h\nu)^2$ versus $h\nu$ for pure and Pt-TiO_2 (b)
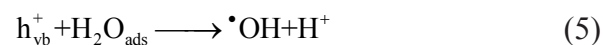
Photocatalytic degradation of AR91 and AY23

The effect of platinum concentration

To study the effect of platinum concentration on degradation of AR91 and AY23, various amount of it, 0.4, 0.6, 0.8, 1.0 and 1.2 wt.% Pt-TiO_2 in the presence of visible-light irradiation was investigated (Figure 5). Results indicate that Pt-TiO_2 is potentially employable for photodegradation processes under visible light. Results of the optical absorption suggest that the presence of platinum on the photocatalyst can significantly influence the optical properties of the TiO_2 photocatalyst and shift the absorption towards the visible range of the spectrum [25]. Results also show the photocatalytic activity of Pt modified TiO_2 on removal of AR91 and AY23, increases with an increase in the Pt-loading and then decreases. Results in Figure 5 show that platinum loading onto TiO_2 surface for removal of AR91 and AY23 has an optimum value of 1%. The experimental results have demonstrated that the presence of platinum loaded onto TiO_2 surface can significantly improved the activity of photocatalysts in the visible range. So the loading of Pt facilitate the absorption of visible light. The metallic Pt,

$Pt(OH)_2$, and PtO_2 deposited on the surface of TiO_2 can significantly absorb visible light. The enhancement of visible optical absorption due to the presence of Pt, $Pt(OH)_2$ and PtO_2 has been proven by UV-vis reflectance spectra [26]. $Pt-TiO_2$ with highest photocatalytic detoxification efficiency compared to TiO_2 (band gap of 3.2 eV). For TiO_2 light below 400 nm is absorbed and capable of generating electron-hole pairs for the photocatalytic process. But for $Pt-TiO_2$ photocatalyst visible light is sufficient for generating electron-hole pairs for the photocatalytic process. As it can be observed from Figure 6, during the photocatalytic process, valence band holes (h_{vb}^+) and conduction band electrons (e_{cb}^-) are generated when aqueous $Pt-TiO_2$ suspension is irradiated with visible light (Eq. 4). The holes at the TiO_2 valence band can oxidize adsorbed water or hydroxide ions to produce hydroxyl radicals (Eqs. 5 and 6).

$$Pt-TiO_2 + h\upsilon > 400 \text{ mm} \rightarrow e_{cb}^- + h_{vb}^+ \qquad (4)$$
$$h_{vb}^+ + H_2O_{ads} \longrightarrow {}^\bullet OH + H^+ \qquad (5)$$
$$h_{vb}^+ + OH_{ads} \longrightarrow {}^\bullet OH \qquad (6)$$

Electron in the conduction band on the catalyst surface can reduce molecular oxygen to superoxide radical anion (Eq. 7). This radical may form hydrogen peroxide (Eq. 8).

$$e_{cb}^- + O_2 \longrightarrow {}^\bullet O_2^- \qquad (7)$$
$${}^\bullet O_2^- + HO_2^\bullet + H^+ \longrightarrow H_2O_2 + O_2 \qquad (8)$$
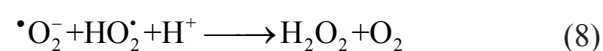
The hydroxyl radical is a powerful oxidizing agent and attacks to organic matters and intermediates (Int.) are formed. These intermediates react with hydroxyl radicals to produce final products (P) (Eq. 9) [30, 36].

$${}^\bullet OH_{ads} + OM \longrightarrow Int. \longrightarrow P \qquad (9)$$
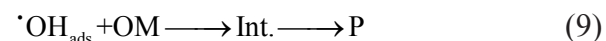
The phenomenon of electron-hole recombination is extremely efficient in the absence of a proper acceptor or donor and hence represents the major energy-wasting step. The photocatalytic activity of TiO_2 can be enhanced by retarding the electron-hole recombination process. Accordingly, the loading of noble metals such as Pt on the TiO_2 surface can expedite the transport of photoexcited electrons to the outer system. Then electrons can reduce molecular oxygen to superoxide radical anion (Eqs. 10 and 11) [37].

$$e_{cb}^- + Pt \rightarrow Pt - e^- \qquad (10)$$
$$Pt - e^- + O_2 \rightarrow Pt + {}^\bullet O_2^- \qquad (11)$$
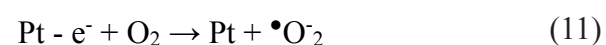
Platinum and other noble metal islands are very effective traps for the excited electrons because of the formation of Schottky barrier at the metal-semiconductor interface which improves the charge separation and thus enhances the photocatalytic activity of TiO_2. The enhancing effect of platinum at degradation of AR91 and AY23 may be

explained by its ability to trap electrons. They act as electron traps. At lower loading level, Pt plays a positive role as electron acceptor, more acceptor centers are provided with increasing Pt loading, therefore the degradation rate for AR91 and AY23 increases with the increase of Pt loading[38]. In contrast, Pt nanoparticles at a higher concentration act as a recombination center and the recombination rate between electrons and holes increases exponentially with the increase of Pt concentration because the average distance between trap sites decreases by increasing the number of Pt nanoparticles. The hyperbolic decrease of the reaction rate with the increased Pt loading on TiO_2 is due to the transfer of photoelectrons from the semiconductor to metal particles and decrease of oxygen concentration photoadsorbed on TiO_2 as negatively charged species for increasing Pt content [32].

By comparing the pseudo-first-order rate constant for pure TiO_2 and Pt-TiO_2 prepared with PD method (Figure 5), it can be clearly observed that the photodegradation rate of AR91 at all percentages of Pt loading is significantly high than that of photodegradation rate of AY23. This may be attributed to the difference in chemical structure of dye. According to the exposition of Khataee and Kasiri [1], photocatalytic process efficiency depends on different parameters, particularly on the chemical structure of the dyes and the nature of functional groups attached on the dye

molecule. To find out the effect of substituent of dyes on photocatalytic process efficiency, the degradation of AR91 and AY23 could be a typical example. This effect has been explored by different researchers. To compare the effect of different substituents on the process rate, Guillard et al. [39] have investigated the degradation of five dyes with different structures and different substitute groups by using UV-irradiated TiO_2 in suspension or supported on glass. They have explained that the higher degradability of Methyl Red could be due to the presence of a carboxylic group which can easily react with H^+ via a photo-Kolbe reaction. However, the presence of a withdrawing group such as SO_3^- is probably at the origin of the less efficient Orange G and Alizarin S degradations. Another suggestion to explain the different reactivity of these dyes could also be their ability to adsorption on TiO_2 surface.

Comparelli et al. [40] have studied the effect of two different substituents in photodegradation of two organic dyes (i.e. Methyl Red and Methyl Orange) in a batch UV/TiO_2 photoreactor with nanocrystal TiO_2 powders. Experiments taken under the best reaction conditions pointed out that the immobilized TiO_2 nanoparticles degraded Methyl Red more quickly than Methyl Orange. This evidence suggests that a precise role must be played by the specific functional group, which differentiates the molecular structure of each dye. In this study,

we have chosen a xanthene dye (AR91) and an azo dye (AY23) with different molecular structures. Since AR91 has a carboxylic group in its structure, this group can easily react with H^+ via a photo-Kolbe reaction, thus the photodegradation rate increases [39] On the other hand, AY23 has two sulfonic groups in its structure. The presence of sulfonic groups in the structure of AY23 retards the photocatalytic degradation efficiency, which can be attributed to decrease of electron density in the aromatic rings and the nitrogen atom of the azo bond [41]. Another reason may be due to photosensitizing reduction mechanism. Epling and Lin [42] reasoned that there must be photosensitized reduction occurred, in such a way that the TiO_2 produced a positive hole. In this case, the photosensitizer (the dye) served as an electron scavenger on the TiO_2 surface, i.e., to produce the positive hole.

$$Dye + h\upsilon > 400 \text{ mm} \rightarrow Dye^* \qquad (12)$$

$$Dye^* + TiO_2 \rightarrow {}^\bullet Dye^- + h^+{}_{vb} \qquad (13)$$
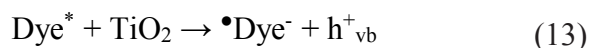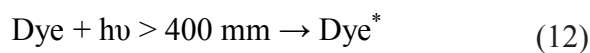
The degradation of the organic dyes could then be mediated by a series of reactions initiated by the hydroxyl radical generated through the oxidation of water molecule by the positive hole (Eq. 5). In this way, we rationalize the experimental observation that AR91 was photodegraded faster than AY23.
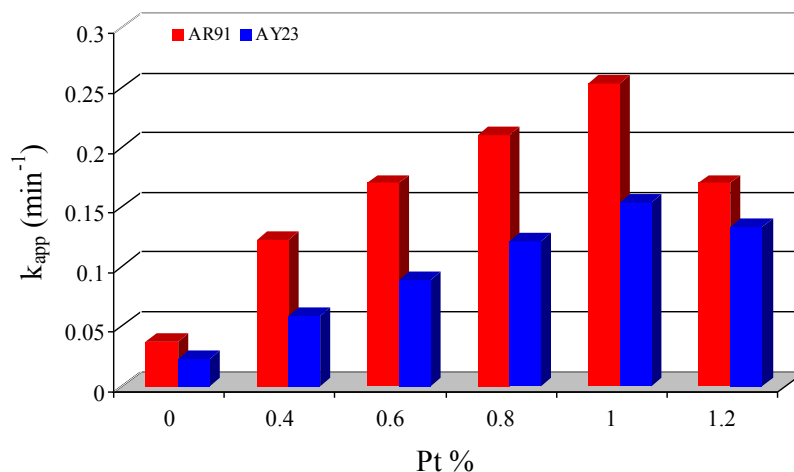

Figure 5. Effect of platinum concentration on the photoactivity of TiO_2 nanoparticles at degradation of AR91 and AY23. I_o=155 klux, [Pollutant]$_o$ = 20 mg/L, [Catalyst] = 600 mg/L.
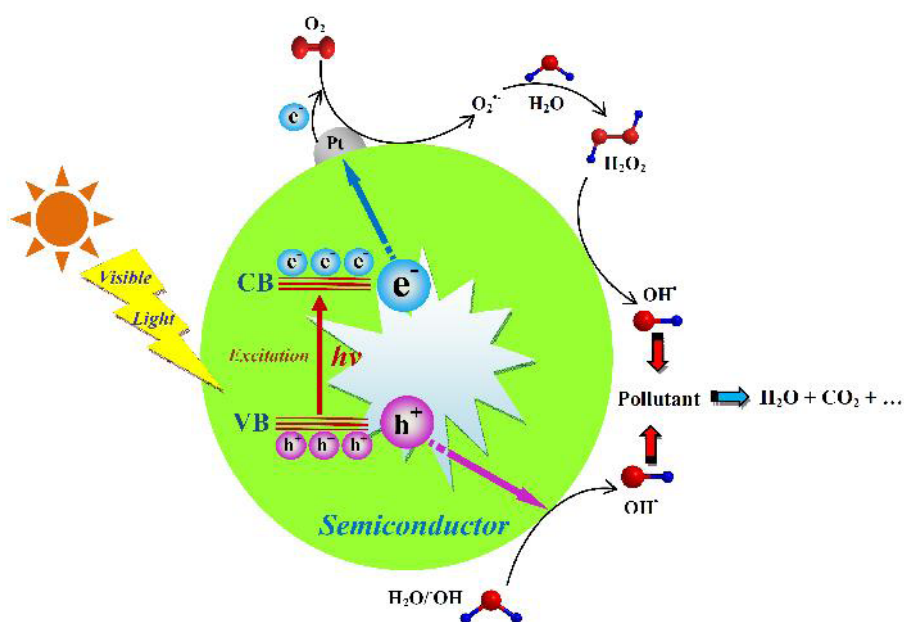
Figure 6. Mechanism of photocatalytic action of Pt-TiO$_2$ nanaoparticles under visible light irradiation.

The effect of photocatalyst dosage

To determine the effect of catalyst dosage, the AR91 and AY23 concentration was fixed at 20 mg/L and the catalyst dosage was varied from 0.0 to 2000 mg/L. Figure 7 shows the effect of catalyst dosage of Pt-TiO$_2$ on the AR91 and AY23 removal. The results demonstrated that Pt-TiO$_2$ has a significant increase of photodegradation rate as compared to the pure TiO$_2$. Compared with pure TiO$_2$, TiO$_2$ modified with 1.0 wt.% (optimum value) of Pt shows that the rate constant increases with increasing the amount of Pt-TiO$_2$ catalyst until 1600 mg/L for AR91 and 1800 mg/L for AY23. The enhancement of the AR91 and AY23 photodegradation rate is due to the increase in active sites available for photocatalytic reaction as the loading of the catalyst is increased. It is obvious that the rate increases with an increase in the amount of catalyst up to a level corresponding to the optimum light absorption [43, 44]. At a higher level of catalyst dosage, although the reactive sites increases, the solution became cloudy and opaque, which reduce the light penetration and lead to the reduction of the availability of active site, while the increase of concentration maybe result in the agglomeration of the catalyst particles, hence the part of the catalyst surface became unavailable for photon absorption and dye adsorption, the decolorization rate subsequently decreases [38]. The obtained results indicated that the photodegradation rate in the presence of all catalysts, is slowed down with AY23 solution in comparison with AR91 solution.
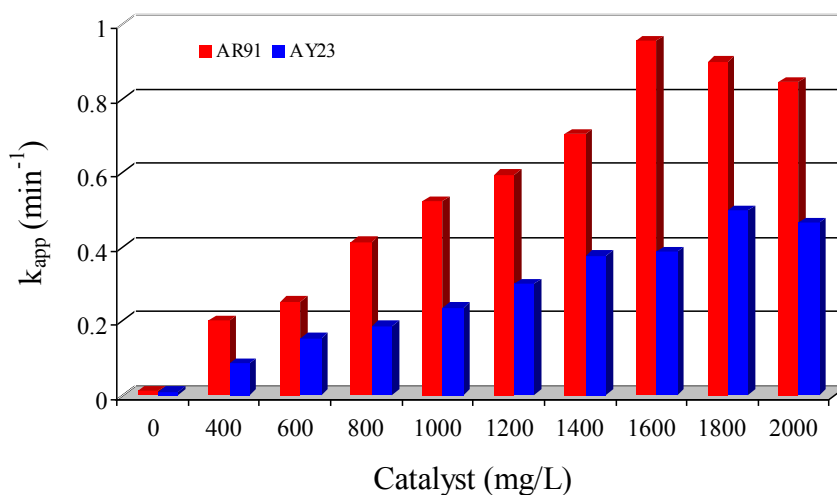
Figure 7. Effect of photocatalyst loading of pure and Pt-TiO$_2$ nanoparticles at degradation of AR91 and AY23. I$_o$=155 klux, [Pollutant]$_o$ = 20 mg/L, 1 wt.% Pt-TiO$_2$ nanoparticles.

The effect of calcination temperature

For the investigation of the effect of calcination temperature on the photocatalytic activity of Pt-loaded TiO$_2$ nanoparticles, the samples were calcined at three different temperatures. As it can be seen in Figure 8, the results showed that with increasing the calcination temperature, the photocalatytic activity of the catalysts were decreased significantly. Pt-TiO$_2$ nanoparticles calcined at 300°C exhibit much higher photocatalytic activity than the samples

calcined at other temperatures. The reasons to be described that the surface area of Pt-TiO$_2$ decreased as the calcinations temperature from 300 to 600°C, and especially the sample calcined at 600°C were almost completely inactive [24]. Reduction in activities of nanoparticles also can be justified due to the increase in crystallite size of nanoparticles, agglomeration of nanoparticles, and transformation of anatase to rutile phase [45, 46].
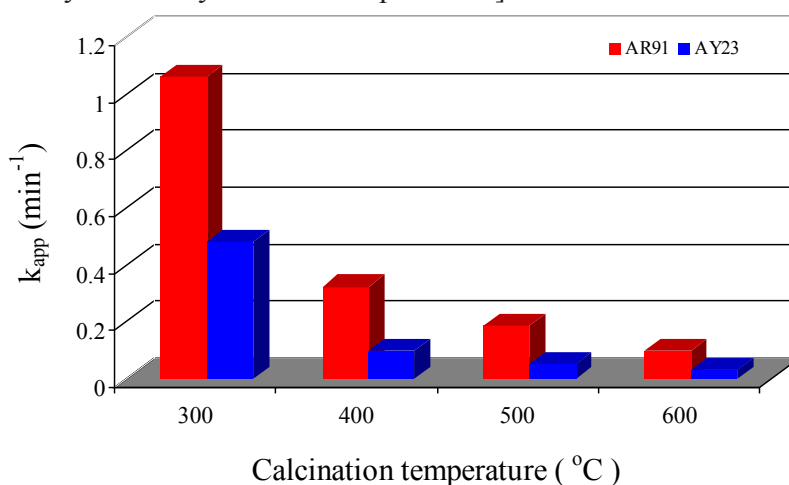

Figure 8. Effect of calcination temperature on photocatalytic activity of Pt-TiO$_2$ nanparticles. I$_o$=155 klux, [Pollutant]o = 20mg/L, 1 wt.% Pt-TiO$_2$ nanoparticles, [Catalyst]$_{AR91}$ = 1600 mg/L, [Catalyst]$_{AY23}$ = 1800 mg/L.

The effect of initial AR91 and AY23 concentration

The initial concentration of AR91 and AY23 in a given catalytic reaction is also another factor which needs to be taken into account. The effect of this factor on the degree of photodegradation was studied by varying the initial concentration over a range of 5-40 mg/L at the optimum conditions. As it can be seen from Figure 9, the results showed that by increasing the dyes concentrations, the photocalatytic activity of the catalysts were decreased significantly. Under visible light irradiation, dye degradation could be controlled by the limited numbers of sites on the surface of photocatalyst. At the same time, hydroxyl radical concentrations decreased since the path length of photons entering the reaction solution decreased, while the initial AR91 and AY23 concentration still increased [47]. Once the concentration of the target pollutant is increased, it also causes the pollutant molecules to absorb light, and photons never reach the catalyst surface and thus, the photodegradation rate decreases [30, 44, 48]. The observed results are in accordance with the fact that as the initial concentration of the dye increases it is the dye rather than Pt-TiO_2 nanoparticles that absorbs the light, which prevents the excitation of the photocatalyst necessary for the efficient photocatalytic degradation process [33]. Shielding the visible light with the high dye concentration may be another reason; thus, the light-triggered catalysts and consequently the concentration of hydroxyl free radicals decreased [49].
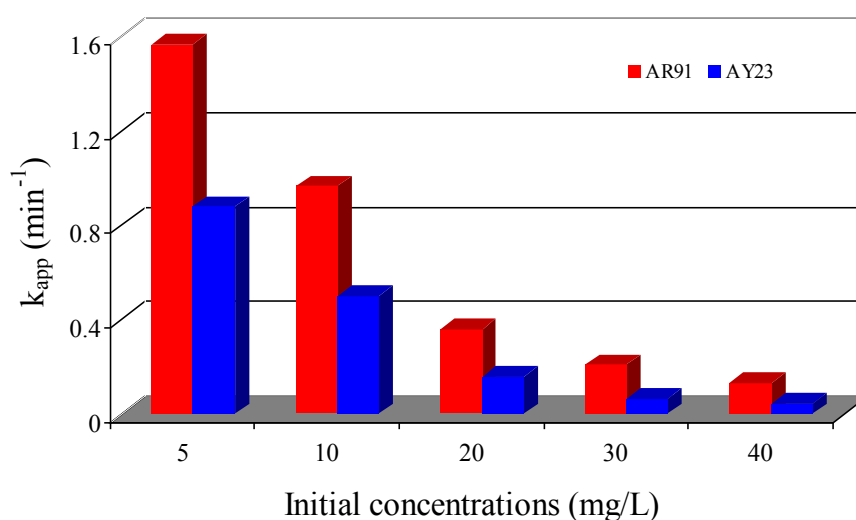

Figure 9. Effect of initial concentration on photocatalytic degradation of AR91 and AY23. I_o=155 klux, 1 wt.% Pt-TiO_2 nanoparticles, [Catalyst]$_{AR91}$ = 1600 mg/L, [Catalyst]$_{AY23}$ = 1800 mg/L.

The effect of visible light intensity

The dependency of pollutant degradation rate on the light intensity has been studied as it can be seen in Figure 10. Reported results indicated that the degradation rate constant of AR91 and AY23 increases as the light intensity increases from 52 to 155 klux. This is because at higher intensity electron hole separation competes with electron hole recombination and results in high reaction rate [50]. The rate of degradation increases when more radiations fall on the catalyst surface and hence more hydroxyl radicals are produced [51, 52].
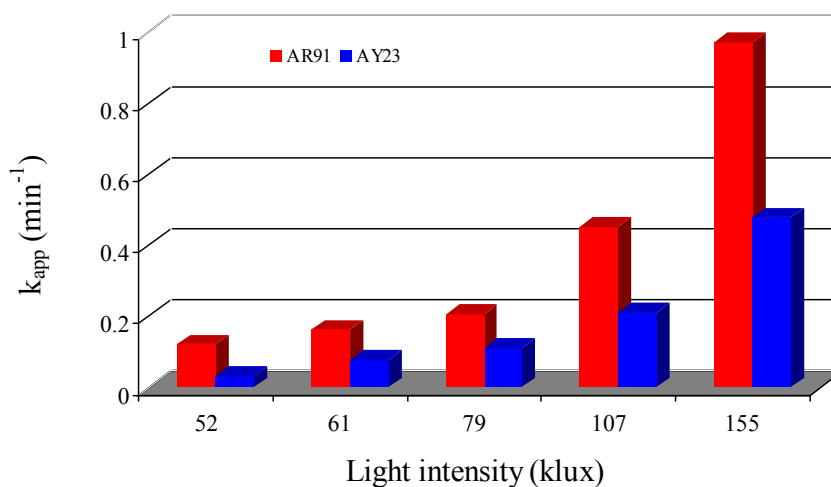

Figure 10. Effect of visible light intensity on the degradation rate constant of AR91 and AY23. [Pollutant]o = 20mg/L, 1 wt.% $Pt-TiO_2$ nanoparticles, [Catalyst]$_{AR91}$ = 1600 mg/L, [Catalyst]$_{AY23}$ = 1800 mg/L.

Photocatalytic mineralization of AR91 and AY23

During the treatment process, the substrate undergoes degradation and forms many intermediate products, which can sometimes be more toxic than the parent compound. Therefore, the complete mineralization of the substrate should be ensured before discharging the polluted waters into the ecosystem. A rather straightforward way of measuring photocatalytic degradation progress of an organic compound is the determination of carbon content of the oxidation product mixture and this can be obtained by monitoring the TOC content of the treated solutions. The TOC data measured for the photocatalytic degradation of AR91 and AY23 at different Pt loadings after 2 h irradiation time at the optimum conditions are presented in Figure 11. The results indicate that the reduction in the TOC value in the presence of 1 Wt.% $Pt-TiO_2$ is significantly higher than other catalysts. The obtained results also indicate that reduction in the TOC value in the presence of all catalysts is lesser than with AY23 solution in comparison with AR91 solution.
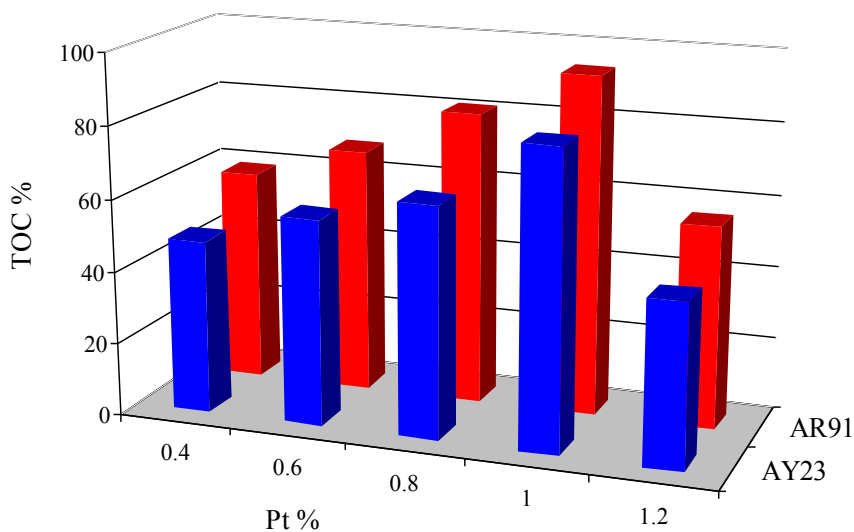
Figure 11. Reduction in the TOC value (%) of AR91 and AY23 solution using Pt-TiO$_2$ catalysts with different Pt loading. [Pollutant]$_o$ = 20mg/L, 1 wt.% Pt-TiO$_2$ nanoparticles, [Catalyst] = 600 mg/L.

Conclusion

Photocatalytic degradation of AR91 and AY23 was studied in the aqueous suspensions of Pt-TiO$_2$ nanoparticles under visible light irradiation. Pt-TiO$_2$ nanoparticles were prepared with PD method and characterized by XRD, SEM, EDX, TEM, and DRS techniques. The DRS results indicated that the deposition of platinum on TiO$_2$ promoted the optical absorption in the visible region and made it possible to be excited by visible light. The study included the investigation of the effect of various parameters, such as platinum concentration, photocatalyst dosage and calcination temperature, initial dye concentration and light intensity. It was found that the 1% Pt content was optimum to achieve the highest efficiency of the AR91 and AY23 photodegradation by the Pt-TiO$_2$ nanoparticles prepared by Pd method. The results showed that the reaction rate of AR91 and AY23 degradation depended on the dosage of Pt-TiO$_2$, showing 1600 mg/L for AR91 and 1800 mg/L for AY23 as the optimum value. Also the best calcinations temperature and light intensity for two dyes was found to be 300 ^{o}C and 155 klux, respectively. By comparing the removal efficiency of AR91 and AY23 at the similar conditions, it was observed that the photodegradation rate of AR91 was faster than that of AY23. The results indicate that the reduction in the TOC value in the presence of all catalysts is lesser than with AY23 solution in comparison with AR91 solution.

Acknowledgments

References

[1] A.R. Khataee, M.B. Kasiri. *J. Mol. Catal. A: Chem*., 328, 8 (2010).

[2] N. Modirshahla, A. Hassani, M.A. Behnajady, R. Rahbarfam. *Desalination*, 271, 187 (2011).

[3] L. Pereira, R. Pereira, C.S. Oliveira, L. Apostol, M. Gavrilescu, M.-N. Pons, O. Zahraa, M.M. Alves. *Photochem. Photobiol*., 89, 33 (2013).

[4] A. Jodat, A. Jodat. *Desal. Wat. Treat*., 52, 2668 (2014).

[5] N. Supaka, K. Juntongjin, S. Damronglerd, M.-L. Delia, P. Strehaiano. *Chem. Eng. J*., 99, 169 (2004).

[6] J.H. Mo, Y.H. Lee, J. Kim, J.Y. Jeong, J. Jegal. *Dyes Pigments*, 76, 429 (2008).

[7] N. Daneshvar, H. Ashassi-Sorkhabi, A. Tizpar. *Sep. Purif. Technol*., 31, 153 (2003).

[8] S. Vasudevan, J. Lakshmi, R. Kamaraj, G. Sozhan. *Asia-Pac. J. Chem. Eng*., 8, 162 (2013).

[9] M. Shokri, A. Jodat, N. Modirshahla, M.A. Behnajady. *Environ. Technol*., 34, 1161 (2013).

[10] D. Chatterjee, S. Dasgupta. *J. Photochem. Photobiol. C: Photochem. Rev.*, 6, 186 (2005).

[11] S.M. Ji, H. Jun, J.s. Jang, H.C. Son, P.H. Borse, J.S. Lee. *J. Photochem. Photobiol. A: Chem.,* 189, 141 (2007).

[12] I. Justicia, G. Garcia, G.A. Battiston, R. Gerbasi, F. Ager, M. Guerra, J. Caixach, J.A. Pardo, J. Riverad, A. Figueras. *Electrochim. Acta*, 50, 4605 (2005).

[13] Q. Ling, J. Sun, Q. Zhou. *Appl. Surf. Sci.*, 254, 3236 (2008).

[14] M.K. Seery, R. George, P. Floris, S.C. Pillai. *J. Photochem. Photobiol. A: Chem.*, 189, 258 (2007).

[15] N. Wang, J. Li, L. Zhu, Y. Dong, H. Tang. *J. Photochem. Photobiol. A: Chem*., 198, 282 (2008).

[16] A.W. Xu, Y. Gao, H.Q. Liu. *J. Catal.*, 207, 151 (2002).

[17] J. Grzechulska, A.W. Morawski. *Appl. Catal*. B, 36, 45 (2002).

[18] Q. Xiao, J. Zhang, C. Xiao, Z. Si, X. Tan. *Sol. Energy*, 82, 706 (2008).

[19] Y. Ishibai, J. Sato, T. Nishikawa, S.h. Miyagishi. *Appl. Catal. B*., 79, 117 (2008).

[20] P.S.S. Kumar, R. Sivakumar, S. Anandan, J. Madhavan, P. Maruthamuthu, M. Ashokkumar. *Water Res*., 42, 4878 (2008).

[21] B. Zhu, K. Li, J. Zhou, S. Wang, S. Zhang, S. Wu, W. Huang. *J. Catal. Commun.*, 9, 2323 (2008).

[22] V. Rodriguez-Gonzalez, S.O. Alfaro, L.M. Torres-Martinez, S.H. Cho, S.W. Lee. *Appl. Catal. B: Environ*., 98, 229 (2010).

[23] M. Pelaez, N.T. Nolan, S.C. Pillai, M.K. Seery, P. Falaras, A.G. Kontos, P.S.M. Dunlop, J.W.J. Hamilton, J.A. Byrne, K. O'Shea, M.H. Entezari, D.D. Dionysiou. *Appl. Catal. B: Environ.,* 125, 331 (2012).

[24] H.W. Chen, Y. Ku, Y.L. Kuo. *Water Res*., 41, 2069 (2007).

[25] H. Katsumata, M. Sada, Y. Nakaoka, S. Co, T. Suzuki, K. Ohta. *J. Hazard. Mater*.,

171, 1081 (2009).

[26] F.B. Li, X.Z. Li. *Chemosphere*, 48, 1103 (2002).

[27] H. Kisch, W. Macyk. *ChemPhysChem*, 3, 399 (2002).

[28] S. Kim, S.K. Lee. *J. Photochem. Photobiol. A: Chem.*, 203, 145 (2009).

[29] S. Kim, S.J. Hwang, W. Choi. *J. Phys. Chem. B,* 109, 24260 (2005).

[30] I.K. Konstantinou, T. Albanis. *J. Appl. Catal. B,* 49, 1 (2004).

[31] S. Chavadej, P. Phuaphromyod, E. Gulari, P. Rangsunvigit, T. Sreethawong. *J. Chem. Eng.*, 137, 489 (2008).

[32] S. Sakthivel, M.V. Shankar, M. Palanichamy, B. Arabindoo, D.W. Bahnemann, V. Murugesan. *Water Res.*, 38, 3001 (2004).

[33] S. Anandan, P. Sathish Kumar, N. Pugazhenthiran, J. Madhavan and P. Maruthamuthu. *Sol. Energ. Mat. Sol.* C, 92, 929 (2008).

[34] A.M. Abdul-Kader. Philos. *Mag. Lett.*, 89, 162 (2009).

[35] R. Ullah, J. Dutta. *J. Hazard. Mater.*, 156, 194 (2008).

[36] E.S. Elmolla, M. Chaudhuri. *Desalination*, 252, 46 (2010).

[37] X. Zhang, F. Zhang, K.-Y. Chan. *Mater. Chem. Phys.*, 97, 384 (2006).

[38] M. Huang, C. Xu, Z. Wu, Y. Huang, J. Lin, J. Wu. *Dyes Pigments*, 77, 327 (2008).

[39] C. Guillard, H. Lachheb, A. Houas, M. Ksibi, E. Elaloui, J.-M. Herrmann. *J.*

Photochem. Photobiol. A: Chem., 158, 27 (2003).

[40] R. Comparellia, E. Fanizza, M.L. Curri, P.D. Cozzoli, G. Mascolo, R. Passino, A. Agostiano. *Appl. Catal. B: Environ*., 55, 81 (2005).

[41] A.R. Khataeea, M.N. Pons, O. Zahraa. *J. Hazard. Mater.*, 168, 451 (2009).

[42] G.A. Epling, C. Lin. *Chemosphere*, 46, 561 (2002).

[43] M.A. Behnajady, N. Modirshahla, N. Daneshvar, M. Rabbani. *Chem. Eng. J.,* 127, 167 (2007).

[44] N. Daneshvar, D. Salari, A.R. Khataee. *J. Photochem. Photobiol. A: Chem.*, 162, 317 (2004).

[45] H.-I. Hsiang, S.-C. Lin. *Ceram. Int.,* 34, 557 (2008).

[46] U.G. Akpan, B.H. Hameed. *J. Hazard. Mater.*, 170, 520 (2009).

[47] H.-Y. Zhu, L. Xiao, R. Jiang, G.-M. Zeng, L. Liu. *Chem. Eng. J.*, 172, 746 (2011).

[48] M.A. Behnajady, N. Modirshahla, R. Hamzavi. *J. Hazard. Mater. B*, 133, 226 (2006).

[49] M.Y. Abdelaal, R.M. Mohamed. *J. Alloys Compd.,* 576, 201 (2013).

[50] B. Pare, B. Sarwan, S.B. Jonnalagadda. *Appl. Surf. Sci.*, 258, 247 (2011).

[51] A.A. Khodja, T. Sehili, J. Pilichowski, P. Boulez. *J. Photochem. Photobiol*. A, 141, 231 (2001).

[52] R. Pourata, A.R. Khatee, S. Aber, N. Daneshvar. *Desalination*, 249, 301 (2009).